ELSEVIER

European Journal of Cardio-thoracic Surgery 29S (2006) S198—S206

EUROPEAN JOURNAL OF CARDIO-THORACIC SURGERY

www.elsevier.com/locate/ejcts

The effect of ventricular sequential contraction on helical heart during pacing: high septal pacing versus biventricular pacing

Hideyuki Tomioka [b], Oliver J. Liakopoulos [b], Gerald D. Buckberg [a,b,*], Nikola Hristov [b], Zhongtuo Tan [b], Georg Trummer [b]

[a] *Option on Bioengineering, California Institute of Technology, Pasadena, CA, USA*
[b] *Department of Surgery, Division of Cardiothoracic Surgery, David Geffen School of Medicine at University of California Los Angeles, 10833 Le Conte Avenue, 62-258 CHS, Los Angeles, CA 90095-1741, USA*

Received 22 February 2006; accepted 28 February 2006

Abstract

Objective: To investigate the effect of biventricular and high septal pacing on the normal contraction sequence of the helical ventricular myocardial band, and its impact on left ventricular function. **Methods:** Ten pigs (25—68 kg) underwent analysis of percent segmental shortening (SS%) by sonomicrometry, with crystals placed along the fiber orientation of the ascending, descending segments, and posterior LV wall within the spatial geometry of the helical heart. Unipolar pacing electrodes stimulated the right atrium (RA) and either the right ventricular apex and left ventricular posterior wall (atrio-biventricular), or the proximal high septum (atrio-high septal). Systemic hemodynamics, QRS-interval, cardiac index (CI), systolic and diastolic LV functions and pressure—dimension loops (*P—D*) were analyzed and cardiac motion was monitored by video analysis. **Results:** Pacing increased normal sinus heart rate (NSR) from 77 ± 9 beats/min to 98 ± 5 beats/min. Atrial pacing did not change the NSR hemodynamic variables. Conversely, atrio-biventricular pacing prolonged the QRS-interval (91 ± 14 ms vs 56 ± 11 ms at baseline, $p < 0.05$) and decreased mean arterial pressure (50 ± 4 mmHg vs 58 ± 12 mmHg), CI (3.4 ± 0.3 L/(min m^2) vs 4.0 ± 0.8 L/(min m^2)) and PRSW (71 ± 25%) compared to NSR ($p < 0.05$). Furthermore, atrio-biventricular pacing decreased SS% in all segments, especially at the LV posterior wall (71% of baseline, $p < 0.05$), and disrupted the NSR shortening sequence (progression from descending to posterior to ascending regions). Changes were characterized by premature stimulation of the posterior wall segment adjacent to the pacer stimulus, with associated (1) decrease of pressure—dimension loop area, (2) desynchronization of *P—D* loops and (3) consistent loss of the twisting pattern of visible cardiac motion. In contrast, atrio-high septal pacing restored systemic hemodynamics, LV systolic and diastolic functions to baseline values and preserved the normal sequence of shortening of the ventricular myocardial band. **Conclusions:** (1) Biventricular pacing disrupts of the natural sequence of shortening of the myocardial band and results in impaired LV function. (2) High septal pacing preserves the sequential shortening pattern of the myocardial band and LV function.

Keywords: Cardiac resynchronization; Septal pacing; Helical myocardial ventricular band; Ventricular function; Helical heart

1. Introduction

Atrio-ventricular pacing is conventionally used to treat bradycardia or heart block because of ease of implantation and electrical stability. Despite returning a normal time-related rhythm, this form of conventional stimulation does not restore hemodynamics. Asynchronous delayed activation of the musculature by ventricular pacing was initially reported by Wiggers [1], and many recent studies confirmed that right ventricular apical (RVA) pacing causes abnormal contraction patterns [2—8]. Recent analysis of the effects of myocyte shortening within the ventricular myocardial band [9] demonstrates how univentricular stimuli initiates a premature impulse at the pacer site, and then disrupts the orderly sequential progression of shortening along the helical heart spatial configuration.

Efforts to offset this hemodynamic limitation of RVA pacing led to use of alternate or multiple pacing sites, especially in patients with congestive heart failure, and outcome results continue to remain inconsistent [10]. One alternate is biventricular activation, termed cardiac resynchronization therapy (CRT), whereby simultaneous pacing of both ventricles confers hemodynamic benefits over those of conventional atrio-monoventricular pacing [11], and is especially useful in the congestive heart failure (CHF) population [12]. This approach is used in failing asynchronous ventricles with [13] and without a wide QRS-interval [14], reduces presystolic mitral regurgitation [15],

* Corresponding author. Address: Department of Surgery, Division of Cardiothoracic Surgery, David Geffen School of Medicine at UCLA, 10833 Le Conte Avenue, 62-258 CHS, Los Angeles, CA 90095-1741, USA. Tel.: +1 310 206 1027; fax: +1 310 825 5895.
E-mail address: gbuckberg@mednet.ucla.edu (G.D. Buckberg).

1010-7940/$ — see front matter © 2006 Published by Elsevier B.V.
doi:10.1016/j.ejcts.2006.02.051

improves quality of life and survival [16], but produces a marginal change in body oxygen uptake [12,17]. Electrical resynchronization initiates a unified current to stimulate contraction, but its effect upon mechanical efficiency to create sequential orderly contraction and twisting has not been evaluated.

A second alternate to direct univentricular approaches of the left or right ventricle muscle is stimulation of the specialized conduction system in the His—Purkinje system to activation of ventricular septum [8,18—21]. This method places the tip of electrode close to the His-bundle, improves cardiac function by synchronous activation and normal muscle contraction sequence and produces ventricular activation maps similar to those from atrial pacing.

The intent of this study is to analyze the effects of biventricular pacing on sequential fiber shortening of the regional components of the myocardial band that underlies the helical heart geometry [22,23]. Function along the rope-like model of the myocardial band will then be compared to stimulation of bundle of His—Purkinje conduction fiber. These fibers exist in the classic anatomic position [24] so that pacer excitation becomes transmitted along the splay of nerve-cable arrangement that exists along the surface of the descending segment of the apical loop. This novel surgical approach to the high septal area shall allow testing that may determine if pacing this region can restore the normal sequential shortening along the apical loop of the helical heart.

A recent univentricular pacing study defined a marked aberration in sequential contraction pattern of the myocardial band with direct left ventricular stimulation [9]. This study will test if this dyssynchrony also occurs with biventricular pacing, and also evaluates if dyssynchrony is avoided by high septal pacing in anesthetized pigs with normal hearts.

2. Materials and methods

All animals received humane care in compliance with the 1996 NRC Guide for the Care and Use of Laboratory Animals, available at: http://www.nap.edu/readingroom/books/lab-rats/contents.html.

The major focus of this study was the comparison of biventricular and high septal pacing on the sequential shortening along the apical loop of the myocardial band.

The experimental protocol is identical to that of the companion paper in this supplement [9]. Briefly, 10 pigs (25—68 kg) underwent endotracheal intubation after anesthesia, and arterial pressure was measured after cannulation of the femoral artery. A Swan—Ganz catheter was inserted into the pulmonary artery via the right jugular vein to measure pulmonary artery pressure (PAP), pulmonary capillary wedge pressure (PCWP) and cardiac output (thermodilution technique). The pericardium was incised after median sternotomy and a solid-stated pressure transducer-tipped catheter (Model MPC-500, Millar Instruments, Inc., Houston, TX, USA) was inserted into the left ventricle to measure LV pressure (LVPsys) and end-diastolic pressure (LVEDP) and its first derivate (dP/dt). Segmental shortening (SS%) of the descending, ascending, and posterior LV segments (Fig. 1) was measured by sonomicrometer crystals (Sonometrics, London, Ont., Canada) and LV volume was obtained using two pairs of crystals oriented across the minor and major axes of the left ventricle (two-axis ellipsoid-based formula) as described previously [9].

2.1. Electrode placement

Unipolar pacing electrodes were positioned at the following locations: the right atrium (RA), the paraseptal right ventricle close to the apex (RV), the posterio-lateral wall of the left ventricle (LV), to simulate the muscular

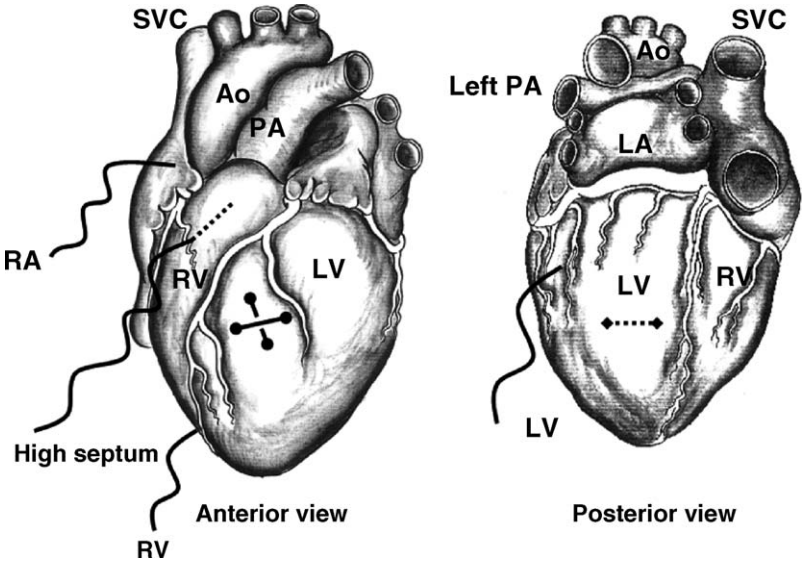

Fig. 1. Schematic anterior and posterior views of the heart showing the different pacing sites and the positioning of the sonomicrometer crystals. Pacing electrodes (wavy lines) were placed at the right atrium (RA), the postero-lateral left ventricular wall (LV) and apex of the right ventricle (RV). The pacing electrode to the high septum was positioned via the right ventricular outflow tract. Crystals were placed into the posterior LV wall (■), and the descending (●—●) and ascending (●- - -●) segments of the LV free wall. Ao.: aorta; LA: left atrium; PA: pulmonary artery; SVC: superior vena cava.

position usually used when left sided pacing leads are placed into a circumflex vein branch reached via catheterization of feeding vessels entering of the coronary sinus. An indifferent electrode was placed on the chest wall in each animal as anode for ventricular pacing.

This anatomic position of the proximal high septum, which normally initiates shortening without pacing, is at the top of the myocardial fold of the descending segment of the apical loop described by Torrent-Guasp. Fig. 2 shows this location in the unfolded heart, and Fig. 3 demonstrates how a unipolar plunge electrode was positioned adjacent to endocardium to reach this His—Purkinje position. This electrode was designed with an insulator that was electrically active only 1 mm from a tip of insulator separation. For insertion, the electrode was placed into a tube cannula that allowed pressure measurements for guidance. Tube insertion followed a transmural course with penetration initiating from (a) the right ventricle, just below the pulmonary artery, (b) going across

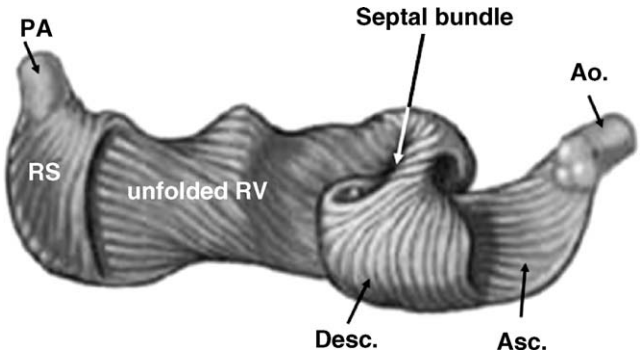

Fig. 2. Schematic drawings of the unfolded ventricular myocardial band as described by Torrent-Guasp. Note visualization of the septum and the location of the bundle of His (septum bundle) that exists after complete unfolding of the basal loop. The right segment (RS), the right ventricular free wall (RV), the ascending segment (Asc.) and the underlying oblique orientated descending segment (Desc.) are identified. Ao.: aorta; PA: pulmonary artery.

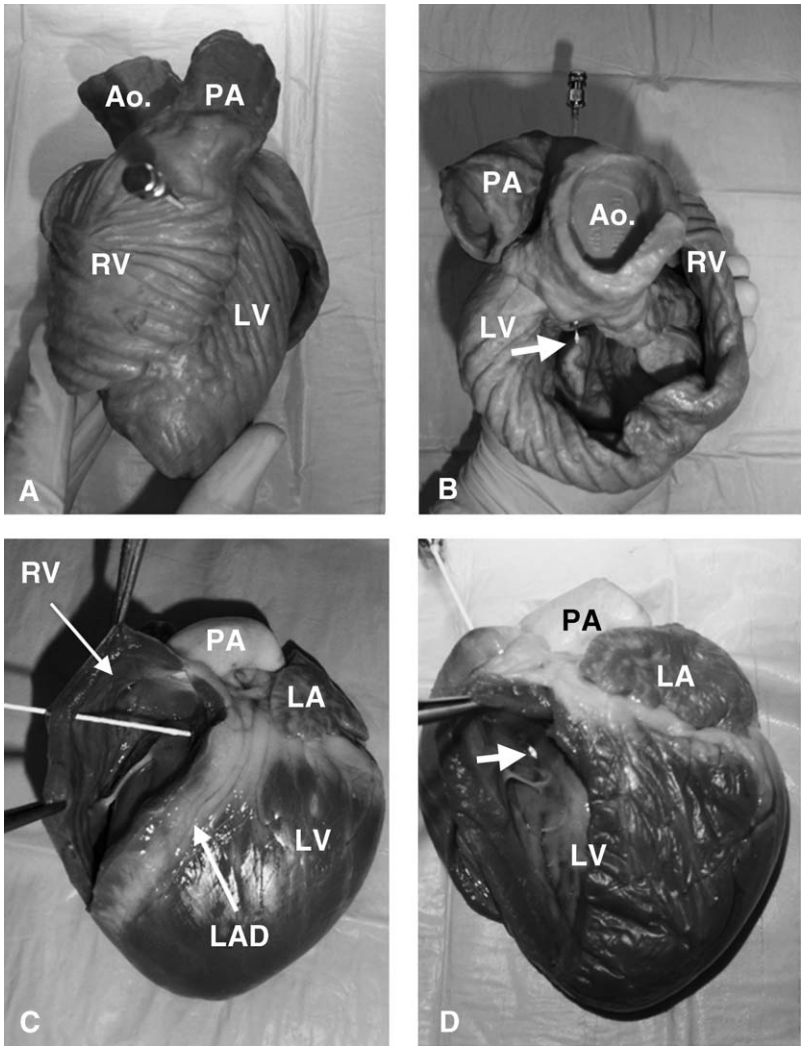

Fig. 3. Images showing the placement septal positioning of the unipolar plunge electrode at the His-bundle in the helical heart model (A and B) and anatomic specimen (C and D). Note that pacing electrode insertion followed a transmural course with penetration initiating from (a) the right ventricle, just below the pulmonary artery (A and C), and (b) going across the septum into the left ventricle thereby leaving the electrode tip position (white arrow) at the septal endocardium (B and D). Correct positioning was confirmed by initiating a pacing stimulus. Ao.: aorta; LAD: left anterior descending artery; LV: left ventricle; PA: pulmonary artery; RV: right ventricle.

the septum into the left ventricle by aspirating oxygenated blood to verify this position, (c) tube withdrawn until no blood returned, thereby confirming tube position just below the septal endocardium, (d) withdrawal of the tube cannula that overlies the plunge electrode, thereby leaving the electrode tip position at the septal endocardium, and finally (e) initiating a pacing stimulus (above resting heart rate) to confirm excitation.

2.2. Pacing protocol

A square-wave constant-voltage electronic stimulator at 2.5 times threshold stimulated the heart. Stimulation parameters (voltage, duration, and frequency) were held constant in each pig, and the mean pacing heart rate for the group was 98 ± 5 beats/min (mean $\pm$ SD). The following pacing interventions were performed in random order: (1) atrial pacing, (2) atrio-biventricular pacing, and (3) atrio-high septal pacing. Atrial pacing was performed by stimulating the right auricular appendage (bipolar) and atrio-monoventricular pacing was performed, making each ventricular electrode unipolar, as done with high septal pacing. Biventricular pacing was performed by using the both ventricular electrodes as the cathode and the skin electrode as the anode. All data were obtained after at least 10 min of each pacing protocol started. The pacing sites were switched after a 10-min pause to assure that hemodynamic parameters had returned to baseline levels.

2.3. Data analysis

During each pacing intervention systemic hemodynamics, systolic and diastolic left ventricular functions, QRS-interval (limb lead II) and segmental shortening (SS%) of each segment were recorded. Percentage of segmental shortening was calculated using following equation:

$$SS\% = \frac{EDL - ESL}{EDL} \times 100,$$

where EDL is end-diastolic shortening and ESL is end-systolic shortening.

LV pressure–volume (P–V) and pressure–dimension (P–D) loops were recorded during transient inferior vena cava occlusions to obtain a series of evenly declining pressure–volume loops. The end-systolic elastance (E_{es}) and preload recruitable stroke work (PRSW) was calculated for each pacing site to analyze myocardial performance independent of loading, geometry, and heart rate [25]. LV performance for each intervention was expressed as a percentage of control before inducing each pacing. In some studies, an octopus traction device was placed on the LV apex, allowing video recordings and analysis of the effectiveness of intrinsic rhythm and pacing modes on ventricular twisting.

2.4. Statistical analysis

Analysis of the data was performed by paired Student's t-tests comparing each intervention with its control. All data were expressed as mean $\pm$ SD. The level of significance was chosen as $p < 0.05$.

3. Results

3.1. Hemodynamics

Hemodynamic data in Table 1 showed that pacing interventions raised heart rate from 77 ± 9 beats/min to 98 ± 5 beats/min ($p < 0.05$). Left ventricular systolic pressure (LVPsys) and cardiac output were maintained during atrial and atrio-high septal pacing, and slightly reduced during atrio-biventricular compared to normal sinus rhythm (NSR). No differences in PAP or PCWP were observed during all pacing interventions. Duration of QRS-interval was similar following atrial and atrio-high septal pacing compared to NSR. Conversely, QRS duration was prolonged from 56 ± 11 ms to 91 ± 14 ms ($p < 0.05$) during atrio-biventricular pacing.

3.2. Left ventricular systolic and diastolic functions

Systolic function (Table 2) showed no difference of peak (+)dP/dt during atrial and atrio-high septal pacing, but atrio-biventricular pacing slightly decreased peak (+)dP/dt. Similarly, end-systolic elastance (Ees) did not differ between NSR, atrial and atrio-high septal pacing, but tended to be lower during atrio-biventricular pacing. PRSW was maintained during atrial and atrio-high septal pacing, but atrio-biventricular pacing reduced PRSW to $71 \pm 21\%$ compared to NSR ($p < 0.05$).

Table 1
Hemodynamic data during sinus rhythm and different pacing sites

	NSR	Atrial pacing	Atrio-biventricular pacing	Atrio-high septal
HR (beats/min)	77 ± 9	$98 \pm 5^{*}$	$98 \pm 5^{*}$	$98 \pm 5^{*}$
QRS int (ms)	56 ± 11	54 ± 10	$91 \pm 14^{*,\#}$	53 ± 9
MAP (mmHg)	58 ± 12	61 ± 9	$50 \pm 4^{*,\#}$	55 ± 4
LVPsys (mmHg)	78 ± 12	79 ± 8	$63 \pm 7^{*,\#}$	72 ± 6
PAPsys (mmHg)	19 ± 3	19 ± 4	18 ± 4	20 ± 3
PCWP (mmHg)	8 ± 3	7 ± 4	8 ± 2	8 ± 2
CI (L/(min m^2))	4.0 ± 0.8	4.4 ± 0.6	$3.4 \pm 0.3^{*,\#}$	4.0 ± 0.2

Hemodynamic data during normal sinus rhythm (NSR) compared to right atrial (RA), atrio-biventricular and atrio-high septal pacing. HR: heart rate; MAP: mean arterial pressure; LVPsys: left ventricular systolic pressure; PAPsys: pulmonary artery systolic pressure; PCWP: pulmonary capillary wedge pressure; CI: cardiac index. All data are mean $\pm$ SD.

* $p < 0.05$ compared to NSR.

$^{\#}$ $p < 0.05$ compared to atrial pacing.

Table 2
Results of pacing interventions on systolic and diastolic functions

	NSR	Atrial pacing	Atrio-biventricular pacing	Atrio-high septal pacing
Peak (+)dP/dt (mmHg/s)	1097 ± 266	1179 ± 187	934 ± 197[#]	1136 ± 128
E_{es} (mmHg/mm)	3.8 ± 1.5	3.8 ± 1.4	3.4 ± 2.8	3.8 ± 1.8
PRSW (%)	100	97 ± 16	71 ± 21[*,#]	82 ± 23
Peak (−)dP/dt (mmHg/s)	−1097 ± 304	−1168 ± 279	−685 ± 139[*,#]	−935 ± 343
LVEDP (mmHg)	14 ± 3	12 ± 3	12 ± 4	13 ± 3

Systolic and diastolic left ventricular functions during normal sinus rhythm (NSR) compared to right atrial (RA), atrio-biventricular and atrio-high septal pacing. Peak (+)dP/dt: peak positive first derivate of LVP; E_{es}: end-systolic elastance; PRSW: preload recruitable stroke work; peak (−)dP/dt: peak negative first derivate of LVP; LVEDP: left ventricular end-diastolic pressure. All data are mean ± SD.

[*] $p < 0.05$ compared to NSR.

[#] $p < 0.05$ compared to atrial pacing.

Diastolic function (Table 2) as expressed by peak (−)dP/dt was similar after NSR, atrial and atrio-high septal pacing. Conversely, atrio-biventricular pacing reduced peak (−)dP/dt from −1097 ± 304 mmHg/s to −685 ± 139 mmHg/s compared to NSR ($p < 0.05$). Pacing interventions had no effect on LVEDP.

3.3. Changes in segmental shortening (SS%)

Percentage of segmental shortening of each segment in Table 3 shows SS% of NSR was maintained following atrial pacing and atrio-high septal pacing. In contrast, atrio-biventricular pacing lowered SS% to 7.5, 16.1 and 29.2 ($p < 0.05$) of baseline values in the descending, ascending, and posterior wall segments.

3.4. Sequential contraction of left ventricle

Normal sinus rhythm resulted in a sequential shortening sequence (Fig. 4), whereby shortening was first initiated in the descending segment, followed (a) ~15 ms later from the LV posterior wall, and (b) ~85 ms later by the ascending segment. Comparison of the sequential shortening sequence with simultaneous ECG and LVP tracings show that (a) descending segment shortening corresponded with the Q-wave and initial slow LVP rise, (b) then followed by posterior wall shortening during the more rapid rise of the LVP curve, and (c) ascending segment shortening which occurred during steep LVP rise and peak (+)dP/dt. A similar time sequence hiatus was observed at the end of shortening, where the descending segment ended shortening first, followed by posterior segment and later by the ascending segment.

Atrial pacing maintained this sequential shortening pattern, but the higher heart rate than NSR decreased time-delay intervals between the three segments (Fig. 5). As previously shown [9], the normal cardiac motion of twisting pattern during NSR (see Video 1 in Ref. [9]) was completely preserved during atrial pacing (see Video 2 in Ref. [9]).

In contrast, biventricular pacing (Fig. 6) disrupted the normal sequence of shortening, where there was a simultaneous beginning of shortening of the descending and posterior segments that began immediately after the ECG pacing spike. Additional disruption existed because end of the shortening sequence began with the posterior wall and was then followed by the descending and ascending segments. The earlier posterior segment shortening initiation existed because the earlier stimulated posterior crystals were adjacent to the posterior LV electrode placement site. The ventricular twisting pattern was lost, as the LV apex bulged following atrio-biventricular stimulation (Video 1).

Conversely, atrio-high septal pacing preserved the normal sequential shortening pattern that occurred following NSR and atrial pacing (Fig. 7). The early initiation of the descending segment shortening was followed by shortening of the posterior wall and ascending segment after 80 ± 16 ms. The start of shortening of the ascending segment occurred during peak (+)dP/dt and rapid rise in the LVP curve to correspond to the normal pattern during NSR and atrial pacing. Furthermore, atrio-high septal pacing preserved the natural time sequence at the end of shortening, and simultaneously restored the natural twisting pattern (Video 2) of ventricular ejection and suction.

3.5. Pressure–dimension loop

Pressure–dimension (P–D) loop during NSR and atrial pacing (Figs. 8 and 9) were identical, whereby (a) the start of contraction of the descending segment occurred during the initial slow LVP rise, (b) posterior wall contraction corresponded to the rise in LVP, and (c) start of shortening in the ascending segment was during the steep rise in LVP. At the

Table 3
Influence of pacing interventions on segmental shortening (SS%)

	NSR	Atrial pacing	Atrio-biventricular pacing	Atrio-high septal pacing
Descending	22.6 ± 5.9	22.1 ± 7.7	20.9 ± 6.2	22.2 ± 6.6
Ascending	14.9 ± 2.7	14.2 ± 2.8	12.5 ± 1.7[*]	14.2 ± 2.7
Posterior	24.3 ± 6.0	23.5 ± 5.2	17.2 ± 5.3[*,#]	20.0 ± 2.4

Percentage of segmental shortening (SS%) during normal sinus rhythm (NSR) compared to right atrial (RA), atrio-biventricular and atrio-high septal pacing. Descending: SS% of the descending segment of the apical loop; ascending: SS% of the ascending segment of the apical loop; posterior: SS% of the posterior wall of the left ventricle. All data are mean ± SD.

[*] $p < 0.05$ compared to NSR.

[#] $p < 0.05$ compared to atrial pacing.

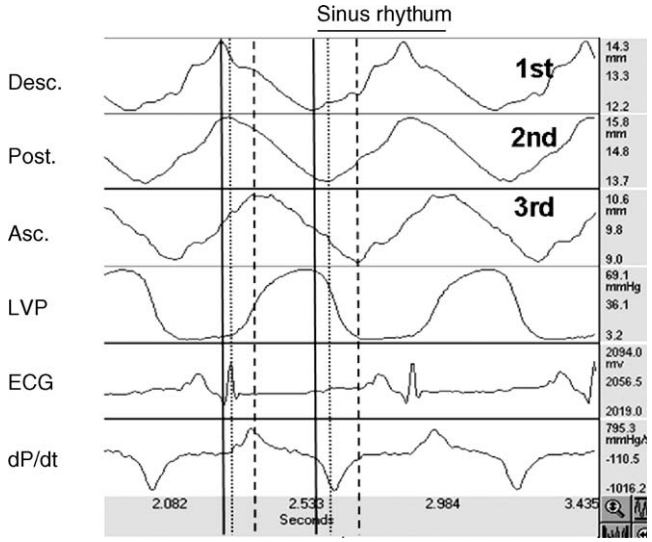

Fig. 4. Simultaneous recordings of sequential shortening of the descending (Desc.), posterior (Post.) and ascending (Asc.) segments during NSR. Note the normal sequence of shortening (a) starts with shortening of the descending segment corresponding to early slow LVP rise, (b) followed by the posterior LV wall shortening, and (c) finally LV ascending segment shortening corresponding with peak positive d*P*/d*t* wave. Furthermore, the end of shortening showed a similar pattern, whereby shortening stopped first at the descending segment, followed by the posterior and then ascending segment. Marking lines indicate the start and end of shortening in the descending segment (solid line), posterior wall (punctuated line) and ascending segment (hatched line). LVP: left ventricular pressure; ECG: electrocardiogram; d*P*/d*t*: first derivate of LVP.

end of contraction the *P—D* loops of the apical loop segments and posterior wall showed a similar timing pattern. The end of shortening was completed first by the descending segment, followed by the LV posterior wall and finally the ascending segment.

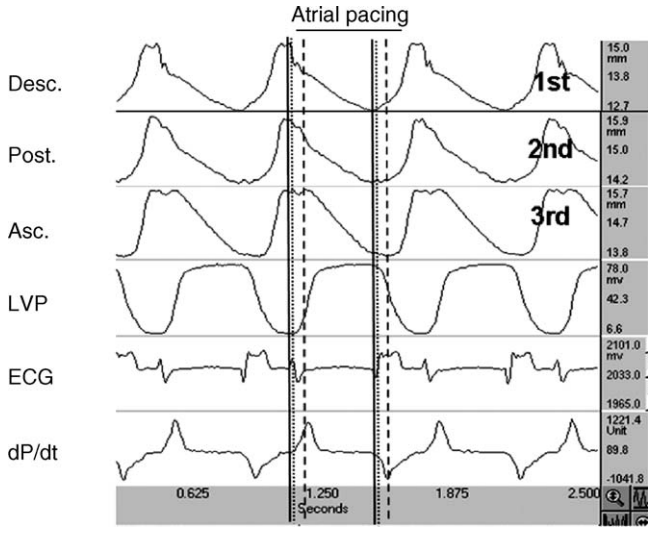

Fig. 5. Simultaneous recordings of sequential shortening of the descending (Desc.), posterior (Post.) and ascending (Asc.) segments during pacing of the right atrium. Note that atrial pacing maintained the sequence of shortening of the segments compared to normal sinus rhythm, with a decrease of time intervals between segments due to a higher heart rate. Marking lines indicate the start and end of shortening in the descending segment (solid line), posterior wall (punctuated line) and ascending segment (hatched line). LVP: left ventricular pressure; ECG: electrocardiogram; d*P*/d*t*: first derivate of LVP.

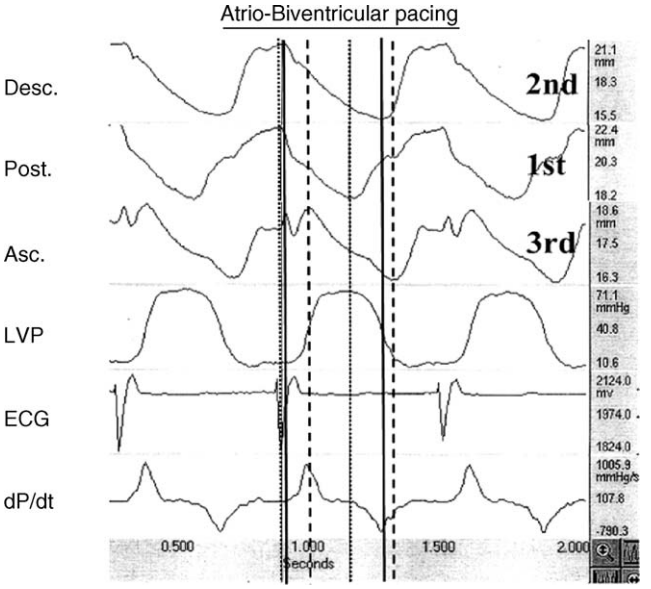

Fig. 6. Simultaneous recordings of sequential shortening of the descending (Desc.), posterior (Post.), and ascending (Asc.) segments during atrio-biventricular pacing. Note the disruption of the normal sequence of shortening, with simultaneous beginning of shortening of the descending and posterior segments that happens immediately after the ECG pacing spike. Similarly, the end of shortening is disrupted since it begins with the posterior wall, and is then followed by the descending and ascending segments. Marking lines indicate the start and end of shortening in the descending segment (solid line), posterior wall (punctuated line) and ascending segment (hatched line). LVP: left ventricular pressure; ECG: electrocardiogram; d*P*/d*t*: first derivate of LVP.

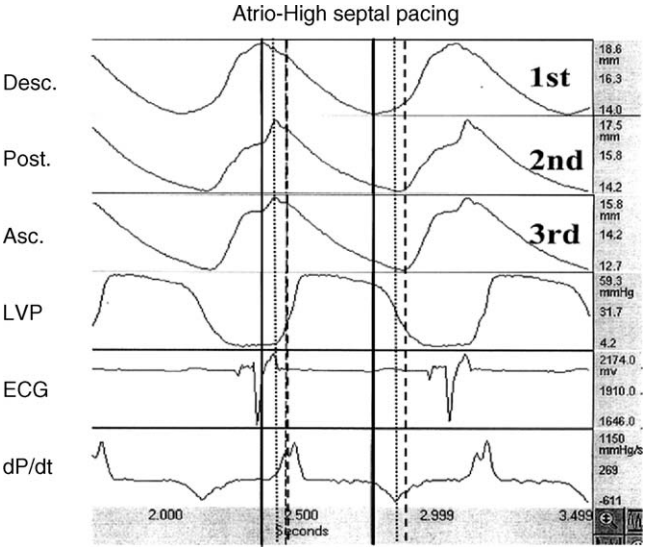

Fig. 7. Simultaneous recordings of sequential shortening of the descending (Desc.), posterior (Post.), and ascending (Asc.) segments during atrio-high septal pacing. Note that atrio-high septal pacing preserved the normal sequential shortening pattern that occurred following NSR and atrial pacing, whereby initiation of shortening begun in the descending segment, followed by posterior wall and then by the ascending segment. Similarly the ascending segment follows this pattern, with the start of shortening corresponding to peak (+)d*P*/d*t* and rapid rise in the LVP curve, and the natural time sequence of end of shortening unaltered from NSR and atrial pacing. Marking lines indicate the start and end of shortening in the descending segment (solid line), posterior wall (punctuated line), and ascending segment (hatched line). LVP: left ventricular pressure; ECG: electrocardiogram; d*P*/d*t*: first derivate of LVP.

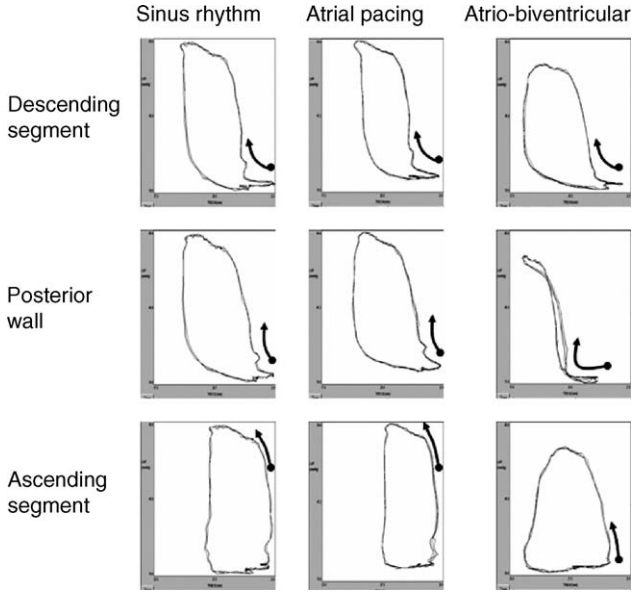

Fig. 8. Comparison of the pressure—dimension (*P—D*) loops of the descending, posterior, and ascending segments during normal sinus rhythm, atrial and atrio-biventricular pacing. The longitudinal axis expresses LV pressure (mmHg), and horizontal axis is segment length (mm). Note that (a) *P—D* loops during NSR and atrial pacing showed a similar pattern, with start of contraction of the descending segment at the beginning of the initial slow rise of LVP, followed by the start of shortening of the LV posterior wall segment and finally the start of contraction of the ascending segment at the end of LVP rise. In contrast biventricular pacing disrupted the normal sequence of shortening with a simultaneous beginning of shortening of the descending and posterior segments, resulting in desynchronized *P—D* loops, especially in the posterior segment.

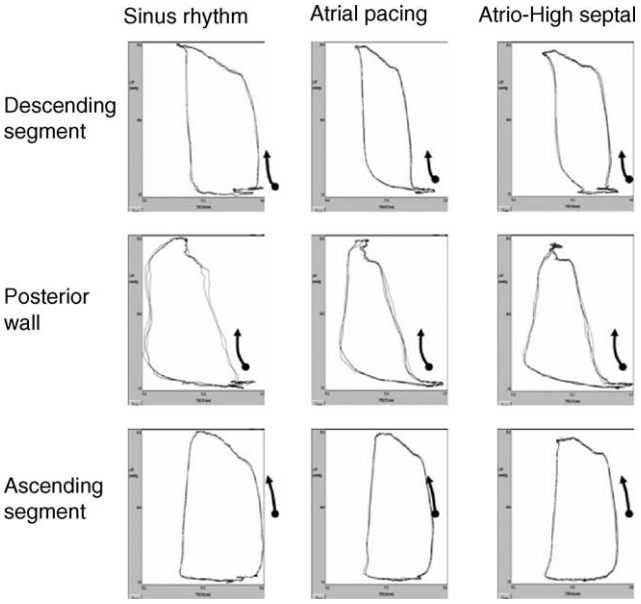

Fig. 9. Comparison of the pressure—dimension (*P—D*) loops of the descending, posterior, and ascending segments during normal sinus rhythm, atrial and atrio-high septal pacing. The longitudinal axis expresses LV pressure (mmHg), and horizontal axis is segment length (mm). Notice that atrio-high septal pacing preserved the normal sequential pattern of shortening and form of *P—D* loops seen during NSR and atrial pacing.

In contrast to the findings during supraventricular rhythm, atrio-biventricular pacing significantly disrupted the normal sequential shortening pattern of the segments which resulted in marked aberrations of *P—D*, especially in the posterior segment (Fig. 8). These aberrations resulted from the early onset of the descending segment and LV posterior wall shortening, thereby causing *P—D* loops that became desynchronized during the early LVP rise interval.

Conversely, atrio-high septal pacing preserved the same *P—D* loops responses observed during NSR and atrial pacing (Fig. 9). The start and end of shortening was first observed in descending segment, followed by posterior wall and finally by ascending segment.

4. Discussion

This study of pacing in normal hearts is a continuation of the prior study [9], that demonstrated that direct univentricular pacing of either the right or left ventricle impaired hemodynamics by causing asynchronous contraction by premature excitation of the muscle beneath the pacer stimulus. The ventricular pacer stimulus disrupted the natural sequential shortening pattern that follows supraventricular stimulation by either sinus rhythm or atrial pacing. This investigation used atrial pacing as a control variable and contrasted atrial-biventricular pacing against atrial-high septal pacing. A novel method of electrode insertion was developed that was based upon knowledge gained from the anatomic geometry of the helical heart model containing the ventricular band described by Torrent-Guasp and co-workers [22,23]. Although biventricular pacing improved hemodynamics compared to univentricular pacing of the left or right ventricles [9], its premature stimulation of the posterior wall disrupted the normal sequence of shortening; an abnormality that was counteracted by high septal pacer stimulation.

The search for alternate pacing sites is not new and was stimulated by the seminal work of Wiggers [1], who defined that asynchrony is produced by transvenous or direct right ventricular apical stimulation. This early observation led to several recent studies demonstrating the superiority of alternate site of multipoint pacing in hemodynamics and cardiac performance [8,11,18—21]. The most common recent intervention is atrial-biventricular pacing, which is used in patients with congestive heart failure [12] who have either normal QRS-intervals [14] or wide QRS-intervals [13] that result from left bundle branch block. The resultant electrical resynchronization allows a more efficient cardiac beat with less strain variation [26].

The findings in this report support the improved hemodynamics of biventricular pacing in normal hearts, compared with greater disruption following univentricular stimulation of the right and left sides [9]. More importantly, recognition of sequencing of normal shortening in the descending, posterior and ascending segments of the myocardial band of the helical heart may be useful to describe why biventricular pacing may improve presystolic mitral regurgitation [15], yet not substantially improve myocardial efficiency since body oxygen uptake is only marginally increased [12,17]. Disruption of the normal patterns of sequential contraction by biventricular pacing

may explain the delay in altering survival during the MIRACLE [27] and COMPANION trials [28]. However, a more recent report altered these adverse findings of no improvement [16].

A novel method of approaching the high ventricular septum was studied to determine the effects of septal pacing on functional responses of fibers that create the cardiac spatial configuration, and to compare these responses to biventricular pacing results. The intent was to initiate a pacer stimulus that restores natural sequencing of shortening. The development of this approach required understanding of the structural elements of the apical loop components of the helical heart, and determining how they affected function within the descending and ascending segments that create the helical vortex at the left ventricular apex.

The natural functional configuration of ejection and suction shown in Video 1 in [9], demonstrates a twisting movement that is associated with a sequential timing and vigor of contraction. Organized action starts with shortening of the descending segment of the apical loop, then proceeds to the posterior segment approximately 14 ± 8 ms later to join in initiation of left ventricular pressure, and is finally followed by shortening of the ascending segment 86 ± 14 ms after the endocardial wall of the left ventricle shortens. Ejection is characterized by co-contraction of all segments corresponding to the rapid phase of LV pressure ascent and the peak (+)dP/dt recording. Dyssynchrony simply means disruption of this organized sequential movement of the successive components of the myocardial band, and resultant avoidance of the normal twisting motion during efficient ejection.

Such disruption follows atrio-biventricular stimulation, and is characterized by reduction of LVP and cardiac index, premature shortening of the posterior segment on the sequential recordings, reduced peak (+)dP/dt, and abnormal P—D loops (Fig. 8) thereby displaying aberrant posterior pressure-segmental lengths. Despite hemodynamic improvement over univentricular pacer recordings [9], the natural sequence is impaired by premature shortening of the paced posterior segment. Video 1 displayed loss of the normal clockwise twisting pattern during ejection, and a similar loss of reciprocal twisting for counterclockwise motion also occurs due to disruption of the normal time course between the end of descending and ascending shortening. Such dyssynchrony likely interferes with vector forces responsible for rapid filling during suction.

Foster et al. [11] demonstrated that atrio-biventricular pacing improved hemodynamic performance compared with the performance observed with conventional atrio-mono-ventricular epicardial pacing after coronary revascularization. Nearly uniform increases in the cardiac index and reductions in the systemic vascular resistance were observed for each patient during atrio-biventricular pacing compared with atrio-monoventricular pacing. However, epicardial activation maps that were constructed during biventricular pacing were never similar to supraventricular rhythms.

While premature stimulation of the posterior wall area causes shortening and resultant transmural contraction, there is no twisting (as shown in Video 1), a similar effect may happen in the septum, which is adjacent to the right ventricular electrode. Such sudden or premature septal shortening moves this central structure into the mid-line, and will thus bring the displaced postero-medial papillary muscle (that is on the septum, as it originates from the descending loop) into a fixed mid-line position. These architectural events will offset the stretch that normally happens when septal contraction is delayed. The consequence of insuring a normal central anatomic septal position is introduction of, a geometric offsetting of tethering of the mitral apparatus that exists during septal bulge or stretching. This architectural effect improves leaflet coaptation, and thus reduces presystolic mitral insufficiency.

The electrically stimulated architectural advantage of a mid-line septum that improves mitral insufficiency will also allow a slight lowering of cardiac end-systolic size [16]. However, no resumption of twisting follows the central septal location induced by biventricular pacing. Absence of return to the normal twisting motion may explain why myocardial efficiency, a value estimated by measuring body oxygen uptake, is not vastly improved [12,17]. Each geometric conclusion about biventricular pacing stimulation stem from recognition of how structure functional relationship of the helical heart is altered by the pacemaker.

The natural pattern of excitation/contraction coupling follows transmission of impulses from the His—Purkinje bundle to the myocyte. Traditional anatomic studies [29,22] show the bundle of His is located at the top of the left ventricular side of the high septum. This position is precisely at the myocardial fold that makes the descending segment of the apical loop have an oblique position. Prior investigators [18,19,21] have activated the high septum by transvenous approaches. Karpawich et al. [19] demonstrated improved acute and long-term hemodynamic effects of proximal septal pacing, stimulating of or close to the septal His—Purkinje specialized conduction system. Takagi et al. [8] showed that ventricular activation maps during proximal septal pacing was (a) similar to those from atrial pacing, and (b) different from those generated during right ventricular outflow tract pacing and right ventricular apex pacing.

The present study used the helical heart model to find a transmural way to excite the high septum from an external source, as may be done in the operating room by using the method developed in this study (Fig. 3). High septal pacing produced shortening by sonomicrometer crystals that was similar to levels observed during NSR and atrial pacing, improved cardiac index more than biventricular pacing and induced the same levels of peak (+)dP/dt, E_{es}, PRSW and peak (−)dP/dt that were observed during supraventricular rhythm. The effective cardiac function was codified by P—D loops that showed how the apical loop descending and ascending segments followed the natural shortening sequence which engenders the organized twisting pattern (Video 2), that displays functional aspects of the myocardial band within the helical heart.

These studies were done in normal hearts, without heart failure, so that clinical implications of this experimental demonstration of high septal pacing must be tested under more abnormal conditions. However, the potential of opening new arenas for identifying the site of complete heart block or for interruption of the left bundle branch, can possibly be achieved by stimulating pacing sites that exists beyond this location; these observations may open chances for future projects in non-dilated hearts. Conversely, asynchrony of contraction exists in dilated hearts without wide QRS-intervals [14]. It is

unlikely that successful electrical stimulation of the high septum will offset this aberrant contraction in dilated hearts, because the electrical abnormality may likely exist within the matrix between the nerves and myocyte [30].

The results of this study lead to the conclusion that fuller understanding of hemodynamic effects of biventricular pacing may evolve by consideration of the structural and functional aspects of the myocardial band of the helical heart. Premature stimulation which causes dyssynchronous contraction by a biventricular source may account for the impaired hemodynamic changes observed when results were compared to supraventricular rhythm from sinus or atrial pacing. A novel approach to high septal pacing was developed by advancing electrodes to septal locations, a stimulation site that was achieved through understanding the helical band geometry. The resultant electrical generation of sequential contraction was restored by pacing the high septal site. The result was resumption of the twisting movement that resembled the classic 1600s descriptions by Borelli [31]. A possible clinical consequence may be introduction of novel techniques to employ electric stimulation to achieve the natural powerful organized sequential contraction that produces high mechanical efficiency during this experimental supraventricular pacer stimulation.

References

[1] Wiggers CJ. The muscular reactions of the mammalian ventricles to artificial surface stimuli. Am J Physiol 1925;73:346—78.

[2] Badke FR, Boinay P, Covell JW. Effects of ventricular pacing on regional left ventricular performance in the dog. Am J Physiol 1980;238(6):H858—67.

[3] Boerth RC, Covell JW. Mechanical performance and efficiency of the left ventricle during ventricular stimulation. Am J Physiol 1971;221(6):1686—91.

[4] Buckingham TA, Candinas R, Attenhofer C, Van Hoeven H, Hug R, Hess O, Jenni R, Amann FW. Systolic and diastolic function with alternate and combined site pacing in the right ventricle. Pacing Clin Electrophysiol 1998;21(5):1077—84.

[5] Burkhoff D, Oikawa RY, Sagawa K. Influence of pacing site on canine left ventricular contraction. Am J Physiol 1986;251(2):H428—35.

[6] Lister JW, Klotz DH, Jomain SL, Stuckey JH, Hoffmann BF. Effect of pacemaker site on cardiac output and ventricular activation in dogs with complete heart block. Am J Cardiol 1964;14:494—503.

[7] Rosenqvist M, Isaaz K, Botvinick EH, Dae MW, Cockrell J, Abbott JA, Schiller NB, Griffin JC. Relative importance of activation sequence compared to atrioventricular synchrony in left ventricular function. Am J Cardiol 1991;67(2):148—56.

[8] Takagi Y, Dumpis Y, Usui A, Maseki T, Watanabe T, Yasuura K. Effects of proximal ventricular septal pacing on hemodynamics and ventricular activation. Pacing Clin Electrophysiol 1999;22(12):1777—81.

[9] Liakopoulos OJ, Tomioka H, Buckberg GD, Tan Z, Hristov N, Trummer G. Sequential deformation and physiological considerations in unipolar right or left ventricular pacing. Eur J Cardiothorac Surg 2006;29S: S188—97.

[10] Varma C, O'Callaghan P, Mahon NG, Hnatkova K, McKenna W, Camm AJ, Rowland E, Brecker SJ. Effect of multisite pacing on ventricular coordination. Heart 2002;87(4):322—8.

[11] Foster AH, Gold MR, McLaughlin JS. Acute hemodynamic effects of atriobiventricular pacing in humans. Ann Thorac Surg 1995;59(2):294—300.

[12] Abraham WT, Young JB, Leon AR, Adler S, Bank AJ, Hall SA, Lieberman R, Liem LB, O'Connell JB, Schroeder JS, Wheelan KR. Effects of cardiac resynchronization on disease progression in patients with left ventricular systolic dysfunction, an indication for an implantable cardioverter-defibrillator, and mildly symptomatic chronic heart failure. Circulation 2004;110(18):2864—8.

[13] Pitzalis MV, Iacoviello M, Romito R, Guida P, De Tommasi E, Luzzi G, Anaclerio M, Forleo C, Rizzon P. Ventricular asynchrony predicts a better outcome in patients with chronic heart failure receiving cardiac resynchronization therapy. J Am Coll Cardiol 2005;45(1):65—9.

[14] Sassara M, Achilli A, Bianchi S, Ficili S, Marullo A, Pontillo D, Achilli P, Peraldo C, Sgreccia F. Long-term effectiveness of dual site left ventricular cardiac resynchronization therapy in a patient with congestive heart failure. Pacing Clin Electrophysiol 2004;27(6):805—7.

[15] Breithardt OA, Sinha AM, Schwammenthal E, Bidaoui N, Markus KU, Franke A, Stellbrink C. Acute effects of cardiac resynchronization therapy on functional mitral regurgitation in advanced systolic heart failure. J Am Coll Cardiol 2003;41(5):765—70.

[16] Cleland JG, Daubert JC, Erdmann E, Freemantle N, Gras D, Kappenberger L, Tavazzi L. The effect of cardiac resynchronization on morbidity and mortality in heart failure. N Engl J Med 2005;352(15):1539—49.

[17] Auricchio A, Stellbrink C, Sack S, Block M, Vogt J, Bakker P, Huth C, Schondube F, Wolfhard U, Bocker D, Krahnefeld O, Kirkels H. Long-term clinical effect of hemodynamically optimized cardiac resynchronization therapy in patients with heart failure and ventricular conduction delay. J Am Coll Cardiol 2002;39(12):2026—33.

[18] Karpawich PP, Perry BL, Farooki ZQ, Clapp SK, Jackson WL, Cicalese CA, Green EW. Pacing in children and young adults with nonsurgical atrioventricular block: comparison of single-rate ventricular and dual-chamber modes. Am Heart J 1987;113(2):316—21.

[19] Karpawich PP, Gates J, Stokes KB. Septal His—Purkinje ventricular pacing in canines: a new endocardial electrode approach. Pacing Clin Electrophysiol 1992;15(11):2011—5.

[20] Raichlen JS, Campbell FW, Edie RN, Josephson ME, Harken AH. The effect of the site of placement of temporary epicardial pacemakers on ventricular function in patients undergoing cardiac surgery. Circulation 1984;70(3):I118—23.

[21] Rosenqvist M, Bergfeldt L, Haga Y, Ryden J, Ryden L, Owall A. The effect of ventricular activation sequence on cardiac performance during pacing. Pacing Clin Electrophysiol 1996;19(9):1279—86.

[22] Buckberg GD, Clemente C, Cox JL, Coghlan HC, Castella M, Torrent-Guasp F, Gharib M. The structure and function of the helical heart and its buttress wrapping. IV. Concepts of dynamic function from the normal macroscopic helical structure. Semin Thorac Cardiovasc Surg 2001;13(4):342—57.

[23] Torrent-Guasp F, Ballester M, Buckberg GD, Carreras F, Flotats A, Carrio I, Ferreira A, Samuels LE, Narula J. Spatial orientation of the ventricular muscle band: physiologic contribution and surgical implications. J Thorac Cardiovasc Surg 2001;122(2):389—92.

[24] Clemente C. Anatomy: a regional atlas of the human body, 4th ed., Urban & Schwartzenberg; 1997.

[25] Glower DD, Spratt JA, Snow ND, Kabas JS, Davis JW, Olsen CO, Tyson GS, Sabiston DC, Rankin JS. Linearity of the Frank—Starling relationship in the intact heart: the concept of preload recruitable stroke work. Circulation 1985;71:994—1009.

[26] Capasso F, Giunta A, Stabile G, Turco P, La RV, Grimaldi G, De Simone A. Left ventricular functional recovery during cardiac resynchronization therapy: predictive role of asynchrony measured by strain rate analysis. Pacing Clin Electrophysiol 2005;28:S1—4.

[27] Young JB, Abraham WT, Smith AL, Leon AR, Lieberman R, Wilkoff B, Canby RC, Schroeder JS, Liem LB, Hall S, Wheelan K. Combined cardiac resynchronization and implantable cardioversion defibrillation in advanced chronic heart failure: the MIRACLE ICD trial. J Am Med Assoc 2003;289(20):2685—94.

[28] Bristow MR, Feldman AM, Saxon LA. Heart failure management using implantable devices for ventricular resynchronization: comparison of medical therapy, pacing, and defibrillation in chronic heart failure (COMPANION) trial. COMPANION Steering Committee and COMPANION Clinical Investigators. J Card Fail 2000;6(3):276—85.

[29] Tawara S. Das Reizleitungssystem des Säugetierherzens: eine anatomisch—histologische Studie über das Atrioventrikularbündel und der Purkinjeschen Fäden Jena, Germany: Gustav Fischer Verlag; 1906.

[30] Coghlan HC, Coghlan AR, Buckberg GD, Gharib M, Cox JL. The structure and function of the helical heart and its buttress wrapping. III. The electric spiral of the heart: the hypothesis of the anisotropic conducting matrix. Semin Thorac Cardiovasc Surg 2001;13(4):333—41.

[31] Borelli GA. In: Bishop LF, Neilson Jr J, editors. History of cardiology. New York: Medical Life Press; 1927.

Appendix A. Supplementary data

Supplementary data associated with this article can be found, in the online version, at doi:10.1016/j.ejcts.2006.02.051.